Solar Phys
DOI 10.1007/s11207-014-0534-6

Coronal Mass Ejections and Non-recurrent Forbush Decreases

A. Belov · A. Abunin · M. Abunina · E. Eroshenko · V. Oleneva · V. Yanke · A. Papaioannou · H. Mavromichalaki · N. Gopalswamy · S. Yashiro

Received: 8 January 2014 / Accepted: 12 April 2014

Abstract Coronal mass ejections (CMEs) and their interplanetary counterparts (interplanetary coronal mass ejections, ICMEs) are responsible for large solar energetic particle events and severe geomagnetic storms. They can modulate the intensity of Galactic cosmic rays, resulting in non-recurrent Forbush decreases (FDs). We investigate the connection between CME manifestations and FDs. We used specially processed data from the worldwide neutron monitor network to pinpoint the characteristics of the recorded FDs together with CME-related data from the detailed online catalog based upon the *Solar and Heliospheric Observatory* (SOHO)/*Large Angle and Spectrometric Coronagraph* (LASCO) data. We report on the correlations of the FD magnitude to the CME initial speed, the ICME transit speed, and

A. Belov · A. Abunin · M. Abunina · E. Eroshenko · V. Oleneva · V. Yanke
IZMIRAN, Russian Academy of Sciences, Moscow, Russia

A. Belov
e-mail: abelov@izmiran.ru

E. Eroshenko
e-mail: erosh@izmiran.ru

A. Papaioannou (✉) · H. Mavromichalaki
Nuclear and Particle Physics Section, Physics Department, National and Kapodistrian University of Athens, Athens, Greece
e-mail: atpapaio@phys.uoa.gr

H. Mavromichalaki
e-mail: emavromi@phys.uoa.gr

A. Papaioannou
IAASARS, National Observatory of Athens, Athens, Greece
e-mail: atpapaio@astro.noa.gr

N. Gopalswamy
NASA/GSFC, Heliophysics Division, Greenbelt, MD 20771, USA
e-mail: Nat.Gopalswamy@nasa.gov

S. Yashiro
The Catholic University of America, Washington, DC, USA

Published online: 25 April 2014

the maximum solar wind speed. Comparisons between the features of CMEs (mass, width, velocity) and the characteristics of FDs are also discussed. FD features for halo, partial halo, and non-halo CMEs are presented and discussed.

Keywords Forbush decreases · Coronal mass ejections · Solar wind · Interplanetary coronal mass ejections · Neutron monitors

1. Introduction

Coronal mass ejections (CMEs) are large-scale solar eruptions during which mass and energy are being released from the Sun to the interplanetary (IP) medium. CMEs are being regularly monitored by white-light coronagraphs at 1 AU onboard the SOHO (Domingo, Fleck, and Poland, 1995) and the *Solar TErrestrial RElations Observatory* (STEREO) missions (Kaiser *et al.*, 2008). The interplanetary counterparts of CMEs (ICMEs) accelerate and/or decelerate during their travel from the Sun to 1 AU because of the interaction with the ambient solar wind (SW). Several studies have shown that fast ICMEs ($V_{\mathrm{CME}} > 400$ km s^{-1}) undergo deceleration because of their interaction with the slower SW, resulting in a decrease of the ICME velocity to that of the ambient SW. On the other hand, slow ICMEs ($V_{\mathrm{CME}} < 400$ km s^{-1}) are accelerated, increasing their velocity from their initial value to the ambient SW velocity $\sim$400 km s^{-1} (Gopalswamy *et al.*, 2000, 2001; Jones *et al.*, 2007; Borgazzi *et al.*, 2008; Démoulin, 2010; Temmer *et al.*, 2011; Shen *et al.*, 2012). This process may be understood as the transfer of momentum between the ICME and the SW, which seems to be fundamentally different for fast and slow ICMEs (compared with the ambient SW velocity) (Borgazzi *et al.*, 2008). By the interaction of fast (slow) moving ICME and the slow (fast) SW, shock waves may be produced (Richardson and Cane, 2011 and references therein). The initial velocity of CMEs upon their detection and the expected ICME velocity recorded *in situ* at Earth are closely connected (Gopalswamy *et al.*, 2000) by an empirical relation (Gopalswamy *et al.*, 2001; Vršnak and Gopalswamy, 2002).

During their travel from the Sun to Earth, CMEs and their corresponding ICMEs interact with Galactic cosmic rays (GCRs) that fill the IP space. The leading shock wave of the ICME (if any) and the following ejecta modulate GCRs, which results in a reduction in the cosmic ray (CR) intensity, known as the Forbush decrease (FD) (Forbush, 1958). FDs are observed at Earth typically with neutron monitors (NMs) because the transient GCR intensity decreases with a relatively fast depression, followed by a slower recovery on a time scale of several days (Forbush, 1958; Lockwood, 1971; Cane, 2000; Belov, 2009; Papaioannou *et al.*, 2010; Jordan *et al.*, 2011). FDs are generally interpreted as the result of CMEs (ICMEs) and/or high-speed SW streams from coronal holes. CMEs (ICMEs) can sometimes reduce the intensity of GCRs at Earth by as much as 20 % and to a lower degree by high-speed streams (HSS) (Belov, 2009). CME-related FDs are referred to as non-recurrent, HSS-related FDs as recurrent (Cane, 2000; Richardson and Cane, 2011). There are several approaches that describe the theoretical background of FDs (Gold, 1959; Parker, 1965; Krymsky *et al.*, 1981; Wibberenz *et al.*, 1998). The registered CR intensity variations are caused by IP shock waves, magnetic clouds, and HSS. Several articles have studied the triggering of FD and CR variability in general (Lockwood, 1971; le Roux and Potgieter, 1991; Cane, 2000; Belov, 2009; Jordan *et al.*, 2011).

2. Motivation

Considering the impact of CMEs/ICMEs on the recorded intensity of GCRs and the production of non-recurrent FDs, it is clear that the CME characteristics (*i.e.* velocity, width, mass) are closely related to those of the FDs (*e.g.* magnitude). Although several studies have focused on case studies (Oh and Yi, 2012; Papaioannou *et al.*, 2013) and others have tried to establish statistical relations based on larger event samples (Richardson and Cane, 2011; Dumbović *et al.*, 2011, 2012), the correlation between FD and CME characteristics has rarely been studied. This is because regular observations of CMEs began only recently in the SOHO era, using the *Solar and Heliospheric Observatory* (SOHO)/*Large Angle and Spectrometric Coronagraph* (LASCO) coronagraphs. SOHO/LASCO observations have been available for all of Solar Cycle 23 and during the current rising phase of Solar Cycle 24, so there is an opportunity to study the FD-CME relationship, which we do in this work.

3. Data Selection

We have used the detailed list of LASCO CMEs available online at http://cdaw.gsfc.nasa.gov/CME_list, which provides a complete coverage of Solar Cycle 23 and the rising phase of Solar Cycle 24. For our analysis it would be ideal to have data on the CME speed toward Earth, on the linear size and the magnetic characteristics of the CME. Such data do not exist, therefore we used available parameters such as the CME onset time, plane-of-the-sky speed and angular width of the CME (Gopalswamy *et al.*, 2009b) that are included in the data base. The CME catalog contains more detailed information on halo CMEs that is available online at http://cdaw.gsfc.nasa.gov/CME_list/halo/halo.html (Gopalswamy *et al.*, 2010a, 2003; Gopalswamy, Yashiro, and Akiyama, 2007). Data for FDs and the IP disturbances have been compiled into a database by the Pushkov Institute of Terrestrial Magnetism, Ionosphere and Radio Wave Propagation (IZMIRAN) cosmic ray group. It includes the results of the global survey method (GSM) (*e.g.* magnitude, decrement, recovery, 3D anisotropy, gradients of the CR) obtained by the data from the worldwide network of NMs throughout the period from 1957 (when continuous observations began) up to the present (Belov, 1987; Belov *et al.*, 2005; Asipenka *et al.*, 2009). This database also includes GOES measurements (continuously updated), the OMNI database IP data, the list of sudden storm commencements (SSCs) from ftp://ftp.ngdc.noaa.gov/STP/SOLAR_DATA/SUDDEN_COMMENCEMENTS/, and solar flares reported in the solar geophysical data, http://sgd.ngdc.noaa.gov/sgd/jsp/solarindex.jsp. The FD database includes all relevant IP data and geomagnetic indices (Kp, Dst). Data on CMEs from 1996 to 2011 (about 17 500 events) and on FDs for the same period (1762 events) were analyzed to explore the connection between FDs and CMEs. This connection was established for a subset of 505 events. Therefore, we selected groups of events based on the degree of identification of the FD event to the parent source (*e.g.* CME). The events in which CMEs are clear related to FDs (the FDs are identified with well-recorded ejections) comprise the 'FD group'.

4. Challenges in the Data Treatment

Although the catalog of SOHO/LASCO CMEs is complete enough, up to date, well organized, and greatly facilitates easy access to the data, one might argue that the infor-

mation provided on each CME is qualitative rather than quantitative. For example, the source regions have not been identified for all CMEs even though associated flare locations are given in the proton, height-time, and X-ray (PHTX) plots for many CMEs. As a rule, the primary direction of the ejection is identified, but it is more qualitative than quantitative because it allows us to distinguish only eastern, western, northern, and southern ejections. Unfortunately, in some cases the information about location of the eruption is not known. As a result and as supporting information, the coordinates of the associated solar flare are often used, quite successfully (Yashiro *et al.*, 2008; Belov *et al.*, 2008). Furthermore, the angular size of CMEs is included in the relevant listings of the catalog (but not in all cases), but this information does not provide a complete picture of the linear size of the CMEs. It is clear that if one selects ejections with the maximum angular sizes (halo), really big ones and rather small but central ejections are included in our sample. Full information on the linear size cannot be extracted even for limb CME events because the angular size depends on the ejection shape. Another point is the provision of data on mass and kinetic energy of CMEs that are included in the CME catalog, but they serve best as an estimation index and are calculated only for a small fraction of limb CME events. The speed of CMEs is most precisely defined at the initial phase of the CME evolution. But it is also difficult to speak about full information on the CME speed, because the velocity of the CME is measured on the plane of the sky. Thus, the most important earthward velocity can only be estimated, and these estimates depend on the model used (Gopalswamy, 2010). Evidently, data on CME acceleration are even less complete and accurate.

This short discussion reveals the challenges and difficulties in trying to find the links between the characteristics of CMEs and FDs. Apparently, we have a deficit of solid quantitative information on CMEs, and for the most important events in our research (central/Earth-directed) this shortcoming is aggravated. These problems may complicate our research efforts, but by no means diminish their need.

5. Results

First, we examined the statistical relation between the basic parameters of CMEs (*i.e.* size, mass, and velocity) and FDs. The CME database includes 17 520 recorded events from 1996 to 2011. During the same time span, 1762 FDs were recorded by NMs on Earth. The connection of FDs with specific CMEs is established for only 505 events. By specific we mean events that we were able to identify and correlate from the CME occurrence to the recorded decrease of the intensity at the NMs at 1 AU.

5.1. CME Velocity as the Driver of FDs

The first physical quantity that we examined is the CME speed for events that present a more pronounced FD than the general population (see Figure 1). The mean speed for FD-associated CMEs is (727 ± 24) km s^{-1}, compared with (405 ± 2) km s^{-1} for the general population (blue-line histogram in Figure 1). Clearly, the FD-associated CMEs are faster than the general population by a factor of two on average. On the other hand, slow CMEs with speeds of ~ 400 km s^{-1} do not result in a pronounced decrease in the NM count rate at Earth. The average speed of FD-associated CMEs is close to that of CMEs associated with magnetic clouds (Gopalswamy *et al.*, 2010a).

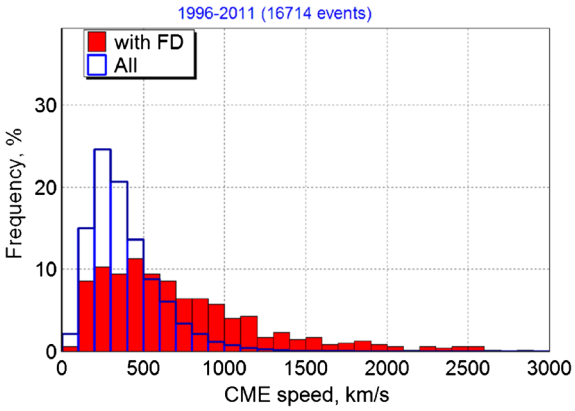

Figure 1 Velocity distribution for all CMEs (□) and for FD-associated CMEs (■) during the period 1996 – 2011 (16 714 events).

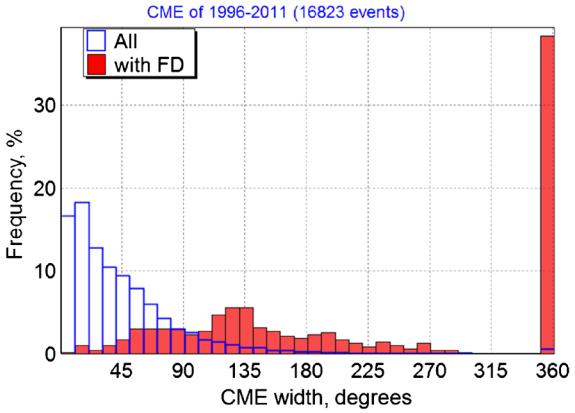

Figure 2 Angular size distribution of CMEs: all CMEs (□) and FD-associated CMEs (■) during the period 1996 – 2011 (16 823 events).

5.2. CME Width as the Driver of FDs

We also examined the CME width as a driver of the FD occurrence. In Figure 2 we present the frequency of events (in %) as a function of the CME angular width (in degrees) for the same categories as before (*i.e.* 'with FD', 'all'). Figure 2 shows that the mean width of FD-associated CMEs is $(220 \pm 6)^\circ$, compared with $(58 \pm 1)^\circ$ for the general population ('all'). This result implies that the larger the angular width of a CME, the higher the possibility of FD occurrence. Interestingly, the fraction of full-halo CMEs is nearly 40 % (see the 360° bin in Figure 2) compared with only about 3 % for the general population (Gopalswamy, 2004). It is well known that the halo CME fraction serves as a measure of the average energy of a CME population (Gopalswamy *et al.*, 2010b). This means that CMEs that cause FDs are generally more energetic, similar to CMEs with interplanetary counterparts detected at 1 AU.

Another conclusion from Figure 2 is that almost all the CMEs in the general population are narrow ejections with angular sizes smaller than 90°. The maximum width in the histogram for the general population falls into the bin 0 – 15°. A completely different picture is observed in the FD group: full-halo (360°) and partial-halo (120 – 270°) CMEs profoundly affect the recorded intensity of GCRs that result in FDs, while the impact of narrower ejections is rather weak.

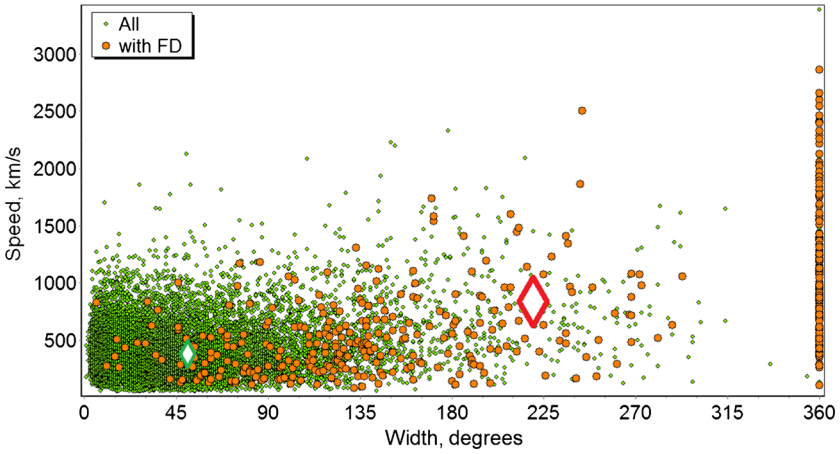

Figure 3 Relation between the angular size and speed of all CME events (●) and the FD-associated subset (●). The diamonds with green and red edges correspond to the average values of the general and FD-associated populations.

5.3. CME Velocity *vs.* Width and FDs

In an attempt to illustrate the effect of both physical quantities in relation to the occurrence of FDs we cross-correlated the CME speed ($\mathrm{km\,s^{-1}}$) and the CME width (degs.) for the FD-associated CMEs and the full population. In Figure 3 the small diamond with green edges shows the relevant CME speed and width in cases where no FD is recorded (*i.e.* (405 ± 2) $\mathrm{km\,s^{-1}}$; $(58 \pm 1)^\circ$), and the larger diamond with red edges indicates the same quantities in cases where FDs have been recorded (*i.e.* (727 ± 24) $\mathrm{km\,s^{-1}}$; $(220 \pm 6)^\circ$). As a result, it is clear that narrow and slow CMEs do not produce FDs, while fast and wide CMEs are needed to produce FDs. This result is also consistent with the fact that faster CMEs are wider (Gopalswamy *et al.*, 2009a).

5.4. CME Mass *vs.* Width and FDs

Next, we compared the CME width (in degrees) with the CME mass (in gr). As can be seen in Figure 4, CMEs with greater mass and width are associated with FDs. This is of course an expected result, since a large-scale structure that can reduce the cosmic-ray intensity should have these features. This result confirms the importance of wider CMEs because wider CMEs are generally known to be more massive (Gopalswamy *et al.*, 2005). Nonetheless, this result is somewhat limited by constraints in the statistics because the mass of the CME is being evaluated in the profile (see the discussion in Section 4 on the limitations imposed by the CME data). Moreover, wider CMEs that are better correlated with FDs (partial-halo or full-halo events) are obviously excluded in Figure 4. Another conclusion that may be drawn from Figure 4 is that CMEs with low mass ($< 10^{13}$ gr) or very high mass ($> 10^{15}$ gr) are not accompanied by FDs. The explanation for this characteristic is that all mass calculations are made for near-limb ejections that usually do not influence the intensity of GCRs at Earth. Mass is not calculated for partial- and full-halo CMEs, which are the basic drivers of FDs. To this end, Figure 4 reveals the limitation of the available data (as discussed in Section 4). Still, a statistical trend is obvious in Figure 4, but we can only identify it for small and not for the most important subset of the events.

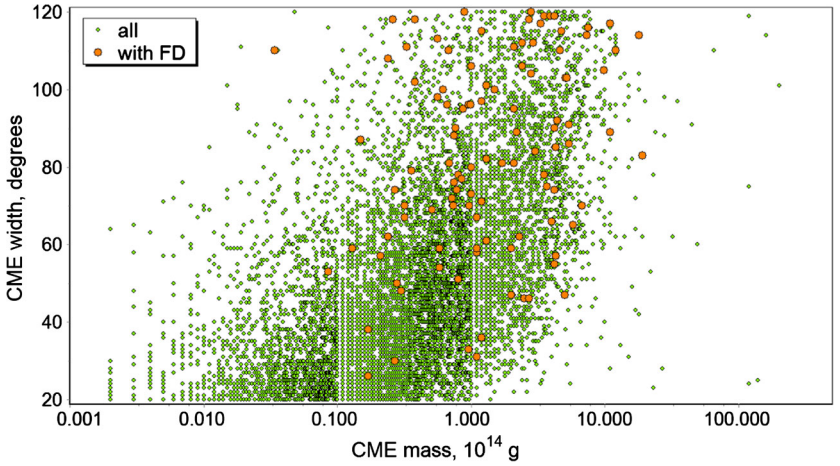

Figure 4 Relation between the mass and angular width of all CME events (●) and the FD-associated subset (●).

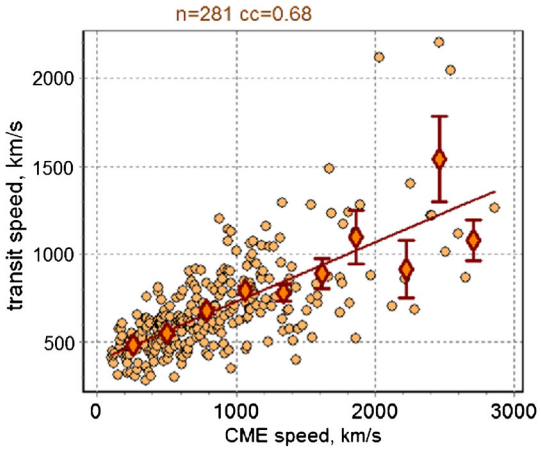

Figure 5 Relation of the Sun to Earth transit speed to the speed of the CME in the plane of the sky near the Sun for events in the FD group. The diamonds represent mean transit speeds calculated (with standard statistical errors) for different intervals of CME speeds. The solid line is the regression line. *n* is the number of events and cc is the correlation coefficient.

5.5. CME Transit Speeds and FDs

Gopalswamy *et al.* (2000) showed that the velocity profile of ICMEs is heavily dependent on the initial speed of CMEs, suggesting that the CME speed defines the ICME speed. Keeping this in mind, we calculated the transit time of the CMEs that resulted in FDs at Earth and compared this with the initial recorded CME speed. As presented in Figure 5, the correlation coefficient is cc = 0.68, which agrees with the outcome reported by Gopalswamy *et al.* (2000). However, the correlation is less than ideal because the initial CME speed does not control the speed changes during the CME propagation in the IP space.

We also explored other possibilities regarding the correlation of the CME initial speed (in km s^{-1}), the transit speed (in km s^{-1}), and the maximum SW speed (in km s^{-1}) recorded at L1 *versus* the magnitude of the FDs (in %). The transit speed (mean velocity of ICME between Sun and Earth) is determined from the difference of the time between the onset of the CME at the Sun and the arrival time of the corresponding ICME at Earth. In Figure 6

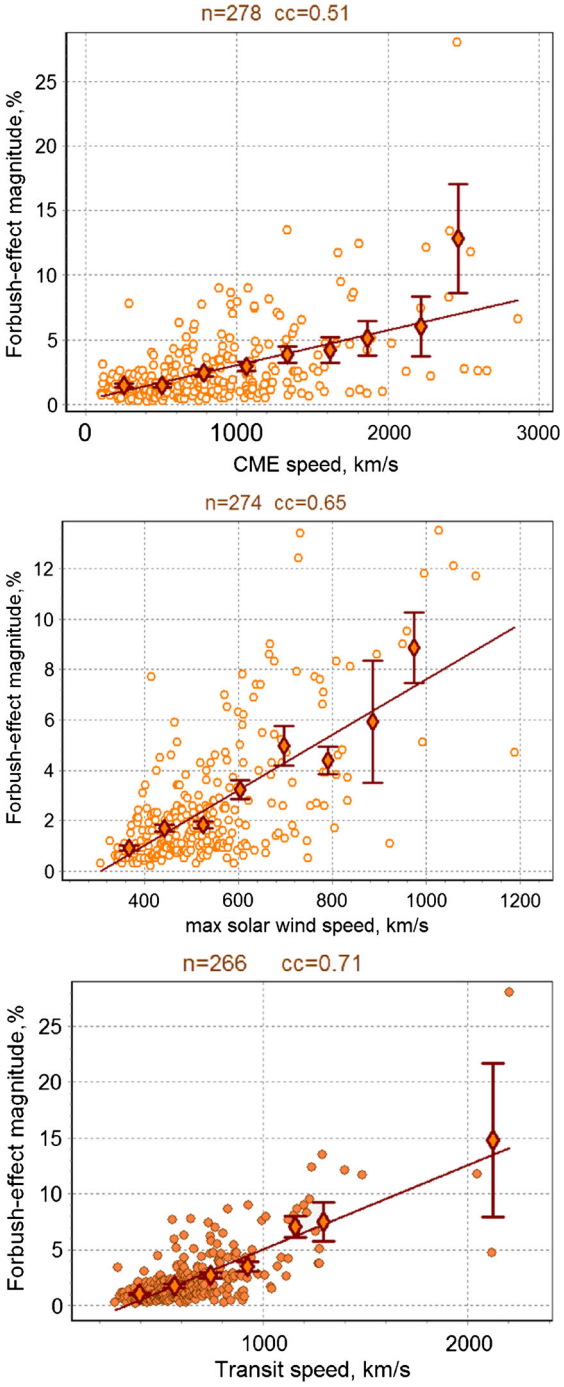

Figure 6 Dependence of the FD magnitude on the speed of the CME (top panel), on the maximum speed of the solar wind inside disturbances measured in near Earth (middle panel), and on the transit speed of the CME (bottom panel). Diamonds are the averaged values of the FDs with standard statistical errors within different CME, solar-wind speed, and transit intervals. *n* is the number of events and cc is the correlation coefficient.

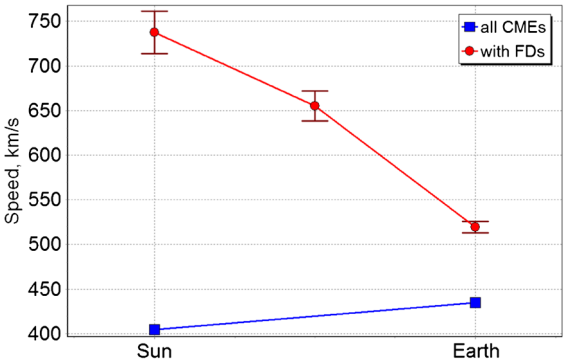

Figure 7 Averaged velocities of CME/ICME near the Sun and Earth in all CME events (■) and in the FD-associated subset (●).

(top panel) the FD magnitude is shown to be correlated with the initial CME speed, with cc = 0.51. The magnitude of the FD has even a better correlation with the CME transit speed with a correlation coefficient of cc = 0.71 (Figure 6, bottom panel). Finally, the magnitude of the FD is also correlated with the maximum SW speed at L1 with cc = 0.65. These three correlations suggest that CMEs cause FDs, but the FDs are not created near the Sun or close to Earth, but instead during the travel time of the CME through the IP medium.

These results are obtained by the GSM (Belov *et al.*, 2005; Asipenka *et al.*, 2009) from the data of CR density variations (the isotropic part of CR variations). This means that the influence of the anisotropy (in particular, daily CR variations) on these connections is in principle excluded. The accuracy of the FD magnitude provided by this method is about 0.1 %. Accordingly, even weak effects ($\approx$0.5 %) seem to be fitted well using the same dependence, and there is no necessity to select and consider them separately.

5.6. ICME Acceleration and/or Deceleration and FDs

As discussed in the introduction, the difference between the velocities of the CMEs released from the Sun into the IP medium and that of the background SW results in the acceleration and/or deceleration of the related ICMEs. Thus far, our next goal was to investigate the dominant characteristic of the ICMEs that produce FDs in comparison with those that do not. Again, we have two categories: 'all CMEs' and those associated with FDs denoted, respectively, by blue squares and red circles in Figure 7. It is clear that the ICMEs that produce FDs suffer deceleration, whereas the CMEs that do not produce FDs are accelerated. This also agrees with the previous results, because the fast and wide CMEs will result in the FDs at Earth, the fast CMEs will be decelerating after interacting with the slow-background SW (Jones *et al.*, 2007). Moreover, the deceleration itself is significant, which shows that the dominant physical process in the motion of the interplanetary ejecta, which results in a significant decrease of the cosmic-ray intensity, is the aerodynamic drag (Vršnak and Gopalswamy, 2002).

From Figure 6 it is clear that the average FD size (in %) increases with the increase in the CME velocity. This is also confirmed in Figure 7, where the average velocity of CMEs and average maximum SW velocity in the corresponding near-Earth disturbance are presented for the group associated with FDs and for all CME events. Because the identification of IP disturbances caused by a certain CME is available only for the selected FD subset, we simply used the average speed of the SW for the entire period of 1996 – 2011 for all CME events. Furthermore, we calculated the average transit speed for the FD subset group (see Figure 6, bottom panel). We see again that the majority of CMEs/ICMEs are slow ejections,

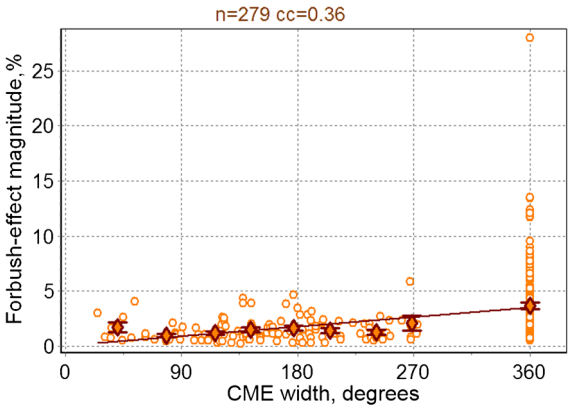

Figure 8 Dependence of the FD magnitude (%) on the angular size (deg) of CMEs. *n* is the number of events and cc is the correlation coefficient.

Table 1 Mean magnitude of the FDs (in %) related to CMEs of different type.

Type of CME	Width (deg)	FD magnitude (%)	No. of events
Halo	360	3.64 ± 0.28	213
Partial halo	120 – 359	1.54 ± 0.11	192
Non halo	< 120	1.01 ± 0.14	131

with their initial speed being, as a rule, lower than the average SW speed. Consequently, they are slightly accelerated during their travel to Earth. In the FD subset group, the initial CME velocity is significantly (almost twice) higher, and these ejections are typically decelerated and thus slowed down during their travel from the Sun to Earth. Nevertheless, the average near-Earth velocity of the ICMEs in the FD subset remains much higher than the average velocity of the quiet SW.

5.7. FD Time Profiles as a Function of the CME Type

We also correlated the FD magnitude with the CME width (deg). As can be seen in Figure 8, the halo CMEs correspond to larger FDs (magnitude up to 28 %). However, it seems that the correlation coefficient is rather low cc = 0.36 and that the CME size as defined by the CME width (in degrees) does not really represent the CME size. As we noted above, the angular width is in the plane of sky, and projection effects can cause the measured size to be very different from the true size. As an example, we note that an angular width of 360° is not the true width of CMEs: halo CMEs are regular CMEs, but projected against the plane of sky (Gopalswamy *et al.*, 2010b). Sometimes, the halo CME can be a combination of ejections of different sizes.

Nonetheless, although limitations exist, there is a clear connection between the type of CME (in terms of angular width) and the corresponding FD magnitude (in %). Table 1 convincingly demonstrates that FDs associated with partial-halo CMEs (width ranging between 120 – 359°) present a higher mean FD magnitude (in %) than FDs associated with CMEs with smaller width ($< 120°$). As expected, the FDs with higher magnitude are associated with halo CMEs (360°). Therefore, halo CMEs are really distinguishable for their impact on GCRs near Earth, as well as for some other effects (Michalek *et al.*, 2006).

We clearly showed the strength of the halo CMEs as an effective modulator of the GCR intensity resulting in FDs with higher magnitude (in %) and at the same time as the driver of

interplanetary and geomagnetic disturbances. It is necessary to emphasize once again that this dependence is not a correlation to the actual size of the CMEs. The angular size (width) of CMEs depends not only on their linear size, but also on the location of the eruption on the solar disk: the closer the CME originates to the center of the solar disk, the larger, as a rule, its angular size. Furthermore, the angular width of an eruption more often reveals the latitudinal size of CMEs (see for example the work by Mierla *et al.*, 2011), whereas for the formation of FDs the azimuthal size is apparently more important. Therefore we conclude that it is no trivial task to identify a relation of the magnitude of the non-recurrent FDs to the actual CME sizes. At present this task has not been done.

6. Discussion and Conclusions

From the analysis that has been carried out in this work, we showed that FD-causing CMEs as a whole are considerably different from the general population of CMEs. CMEs associated with FDs are characterized by significantly higher velocity, wider angular sizes, and larger mass. Thus, the correlations of the CME characteristics (especially their velocity and angular size) to the FD magnitude allowed us to estimate the expected efficiency of CMEs as the modulator of GCRs that result in FDs at 1 AU.

It is evident from our analysis that the largest FDs are created by large CMEs that are characterized by high velocity and large width. It is therefore natural to assume that all large CMEs modulate GCRs – significantly – and create FDs in the inner heliosphere. But we can only observe part of all the effects of this kind, since they occur far from Earth (for details see the work of Eroshenko *et al.*, 2009 and Papaioannou *et al.*, 2009). This latter fact and the objective difficulties in the quantitative description of CMEs, as furnished in this study, impose certain restrictions on the applicability of the relations found. Apparently, for the problem CME – FD it is reasonable not to limit ourselves only to the direct observations of CMEs, but also to inspect related data, for example, lower-coronal observations of eruptions (Chertok *et al.*, 2013).

It is clear that any in-depth research of FDs is impossible without studying CMEs; this is well accepted by the scientific community. Our analysis has also shown that FDs can be a very useful asset for CME analyses. For example, one of the problems in studying CMEs is the absence of any general characteristic of their power (which is similar to the importance of X-ray flares), allowing us to compare the expected efficiency of CMEs in the IP space, the modulation of GCRs, and the geomagnetic field. Such an integral characteristic should probably be searched for beyond the CME parameters. One of the most promising candidates for this is the FD magnitude.

Acknowledgements The SOHO/LASCO/CME catalog is generated and maintained at the CDAW Data Center by NASA and The Catholic University of America in cooperation with the Naval Research Laboratory. SOHO is a project of international cooperation between ESA and NASA. The work of coauthors N. Gopalswamy and S. Yashiro is supported by NASA's LWS TR & T program. The authors would like to thank the anonymous referee for the careful evaluation of the manuscript.

References

Asipenka, A., Belov, A., Eroshenko, E., Klepach, E., Oleneva, V., Yanke, V.: 2009, *Adv. Space Res.* **43**, 708.
Belov, A.V.: 1987 In: *Proc. 20th Int. Cosmic Ray Conf.* **4**, 119.
Belov, A.V.: 2009, In: Gopalswamy, N., Webb, D. (eds.) *Proc. IAU Symp.* **257**, Cambridge University Press, Cambridge, 439.

Belov, A.V., Eroshenko, E., Oleneva, V., Yanke, V.: 2008, *J. Atmos. Solar-Terr. Phys.* **70**, 342.
Belov, A.V., Baisultanova, L., Eroshenko, E., Yanke, V., Mavromichalaki, H., Plainaki, C., Mariatos, G., Pchelkin, V.: 2005, *J. Geophys. Res.* 110. DOI.
Borgazzi, A., Lara, A., Romero-Salazar, L., Ventura, A.: 2008, *Geofís. Int.* **47**, 301.
Cane, H.: 2000, *Space Sci. Rev.* **93**, 55.
Chertok, I.M., Grechnev, V.V., Belov, A.V., Abunin, A.A.: 2013, *Solar Phys.* **282**, 175.
Démoulin, P.: 2010 In: *12th Int. Solar Wind Conf., AIP Conf. Proc.* **1216**, 329.
Domingo, V., Fleck, B., Poland, A.I.: 1995, *Solar Phys.* **162**, 1.
Dumbović, M., Vršnak, B., Čalogović, J., Karlica, M.: 2011, *Astron. Astrophys.* **531**, A91.
Dumbović, M., Vršnak, B., Čalogović, J., Župan, R.: 2012, *Astron. Astrophys.* **538**, A28.
Eroshenko, E., Belov, A., Mavromichalaki, H., Oleneva, V., Papaioannou, A., Yanke, V.: 2009, In: Gopalswamy, N., Webb, D. (eds.) *Proc. IAU Symp.* **257**, Cambridge University Press, Cambridge, 451.
Forbush, S.E.: 1958, *J. Geophys. Res.* **63**, 651.
Gold, T.: 1959, *J. Geophys. Res.* **64**, 1665.
Gopalswamy, N.: 2004, In: Poletto, G., Suess, S.T. (eds.) *The Sun and the Heliosphere as an Integrated System, Astrophys. Space Sci. Lib.* **317**, 201.
Gopalswamy, N.: 2010, In: Dorotović, I. (ed.) *Proc. of the 20th Slovak National Solar Physics Workshop, Slovak Central Observatory* **1**, 108.
Gopalswamy, N., Yashiro, S., Akiyama, S.: 2007, *J. Geophys. Res.* **112**, A06112.
Gopalswamy, N., Lara, A., Lepping, R.P., Kaiser, M.L., Berdichevsky, D., St. Cyr, O.C.: 2000, *Geophys. Res. Lett.* **27**, 145.
Gopalswamy, N., Lara, A., Yashiro, S., Kaiser, M.L., Howard, R.A.: 2001, *J. Geophys. Res.* **106**(A12), 29207.
Gopalswamy, N., Lara, A., Yashiro, S., Nunes, S., Howard, R.A.: 2003 In: *Proc. of Solar Variability as an Input to the Earth's Environment, ESA-SP* **1**, 403.
Gopalswamy, N., Aguilar-Rodriguez, E., Yashiro, S., Nunes, S., Kaiser, M.L., Howard, R.A.: 2005, *J. Geophys. Res.* **110**, A12S07.
Gopalswamy, N., Dal Lago, A., Yashiro, S., Akiyama, S.: 2009a, *Cent. Eur. Astrophys. Bull.* **33**, 115.
Gopalswamy, N., Yashiro, S., Michalek, G., Stenborg, G., Vourlidas, A., Freeland, S., Howard, R.: 2009b, *Earth Moon Planets* **104**, 295.
Gopalswamy, N., Akiyama, S., Yashiro, S., Mäkelä, P.: 2010a, In: Hasan, S.S., Rutten, R.J. (eds.) *Magnetic Coupling Between the Interior and Atmosphere of the Sun, Astrophys. Space Scien. Proc.* **1**, 289.
Gopalswamy, N., Yashiro, S., Michalek, G., Xie, H., Mäkelä, P., Vourlidas, A., Howard, R.: 2010b, *Sun Geosphere* **5**, 7.
Jones, R.A., Breen, A.R., Fallows, R.A., Canals, A., Bisi, M.M., Lawrence, G.: 2007, *J. Geophys. Res.* **112**, A08107. DOI.
Jordan, A.P., Spence, H.E., Blake, J.B., Shaul, D.N.A.: 2011, *J. Geophys. Res.* **116**, A11103. DOI.
Kaiser, M.L., Kucera, T.A., Davila, J.M., St. Cyr, O.C., Guhathakurta, M., Christian, E.: 2008, *Space Sci. Rev.* **136**, 5.
Krymsky, G.F., Kuzmin, A.I., Krivoshapkin, P.A., Samsonov, I.S., Skripin, G.V., Transkii, I.A., Chirkov, N.P.: 1981, *Cosmic Rays and Solar Wind*, Nauka, Novosibirsk.
le Roux, J., Potgieter, M.: 1991, *Astron. Astrophys.* **243**, 531.
Lockwood, J.A.: 1971, *Space Sci. Rev.* **12**, 658.
Michalek, G., Gopalswamy, N., Lara, A., Yashiro, S.: 2006, *Space Weather* **4**, S10003.
Mierla, M., Inhester, B., Rodriguez, L., Gissot, S., Zhukov, A., Srivastava, N.: 2011, *J. Atmos. Solar-Terr. Phys.* **73**, 1166.
Oh, S.Y., Yi, Y.: 2012, *Solar Phys.* **280**, 197.
Papaioannou, A., Belov, A., Mavromichalaki, H., Eroshenko, E., Oleneva, V.: 2009, *Adv. Space Res.* **43**, 582.
Papaioannou, A., Malandraki, O.E., Belov, A., Skoug, R., Mavromichalaki, H., Eroshenko, E., Abunin, A., Lepri, S.: 2010, *Solar Phys.* **266**, 181.
Papaioannou, A., Belov, A.V., Mavromichalaki, H., Eroshenko, E., Yanke, V., Asvestari, E., Abunin, A., Abunina, M.: 2013, *J. Phys. Conf. Ser.* **409**, 012202.
Parker, E.: 1965, *Planet. Space Res.* **13**, 9.
Richardson, I.G., Cane, H.V.: 2011, *Solar Phys.* **270**, 609.
Shen, F., Wu, S.T., Feng, X., Wu, C.-C.: 2012, *J. Geophys. Res.* **117**, A11101. DOI.
Temmer, M., Rollett, T., Möstl, C., Veronig, A.M., Vršnak, B., Odstrčil, D.: 2011, *Astrophys. J.* **743**, 101.
Vršnak, B., Gopalswamy, N.: 2002, *J. Geophys. Res.* **107**, A21019.
Wibberenz, G., Le Roux, J., Potgieter, M., Bieber, J.: 1998, *Space Sci. Rev.* **83**, 309.
Yashiro, S., Michalek, G., Akiyama, S., Gopalswamy, N., Howard, R.A.: 2008, *Astrophys. J.* **673**, 1174.